https://doi.org/10.5194/egusphere-2022-525
Preprint. Discussion started: 13 July 2022
© Author(s) 2022. CC BY 4.0 License.

Air-sea gas exchange in a seagrass ecosystem

Ryo Dobashi[1], David T. Ho[1]

[1]Department of Oceanography, University of Hawai'i at Mānoa, 1000 Pope Road, Honolulu, Hawaii 96822, USA

Correspondence to: Ryo Dobashi (rdobashi@hawaii.edu)

Abstract. Seagrass meadows are one of the most productive ecosystems in the world and could play a role in mitigating the increase of atmospheric CO_2 from human activities. Understanding their role in the global carbon cycle requires knowledge of air-sea CO_2 fluxes and hence knowledge of the gas transfer velocity. In this study, gas transfer velocity and its controlling processes were examined in a seagrass ecosystem in south Florida. Gas transfer velocity was determined using the ^3He and SF_6 dual tracer technique in Florida Bay near Bob Allen Keys (25.02663°N, 80.68137°W) between 3 and 8 April 2015. The observed gas transfer velocity normalized for CO_2 in freshwater at 20° C, $k(600)$, was 4.8 ± 1.8 cm h^{-1}. The result gas transfer velocities were lower than previous experiments in the coastal and open oceans at the same wind speeds. Therefore, using published wind speed/gas exchange parameterizations would overpredict gas transfer velocities and CO_2 fluxes in this area. The deviation in $k(600)$ from other settings was weakly correlated to tidal motion and air-sea temperature difference, implying that wind is the dominant factor driving gas exchange. The lower gas transfer velocity was most likely due to wave attenuation by seagrass and limited wind fetch in this area. A new wind speed/gas exchange parameterization is proposed ($k(600) = 0.125u_{10}^2$), which might be applicable to other seagrass ecosystems and wind fetch limited environments.

1 Introduction

Seagrass meadows are one of the most productive areas in the world, and they stock as much as 4.2–8.4 PgC in the soil (Fourqurean et al., 2012). Because much of the organic carbon produced via photosynthesis sink to the bottom, seagrass meadows are expected to be blue carbon sinks that can help mitigate the increase of anthropogenic CO_2. Duarte et al. (2005) showed that seagrasses bury 27.4 Tg C y^{-1}, which is about 10 % of the total ocean carbon burial. Recently, the role of seagrasses in the global carbon cycle has been revisited, as the CO_2 emission from $CaCO_3$ production was found to be large (Howard et al., 2017; Van dam et al., 2021). Howard et al. (2017) examined the stock of organic and inorganic carbon in the soil of Florida Bay and southeastern Brazil, and found that the soils in both regions have more inorganic carbon than organic carbon and are sources of CO_2 to the atmosphere.

Knowledge of the gas transfer velocity (k) is needed to understand the role of seagrass ecosystems in the global carbon cycle, since air-sea CO_2 flux is a function of k and the air-sea difference in the partial pressure of CO_2 (pCO_2). Because k is

https://doi.org/10.5194/egusphere-2022-525
Preprint. Discussion started: 13 July 2022
© Author(s) 2022. CC BY 4.0 License.

difficult to measure, it is often parameterized by easily and widely measured parameters such as wind speed. In deep offshore regions, wind is known to predict the gas transfer velocity well since wind creates waves and currents, which control turbulence and bubbles at the sea surface (Wanninkhof et al., 2009). On the other hand, in shallow regions, other parameters become important as well (e.g., Ho et al., 2016; 2018a). Ho et al. 2016 showed that gas transfer velocity could be estimated well by wind speed and current speed in a shallow tidal estuary in south Florida, because the current enhances bottom-generated turbulence.

In Florida Bay, k has been estimated from commonly used wind speed/gas exchange parameterizations. Zhang and Fischer (2014) determined the air-sea CO_2 flux to be 3.93 ± 0.91 mol m^{-2} yr^{-1} in Florida Bay using the wind speed/gas exchange parameterization of Wanninkhof (1992). Van Dam et al. (2020) estimated k by using heat as a proxy (k_H) in Florida Bay and found that k_H is lower compared with k derived from published wind speed/gas exchange parameterizations when wind shear is relatively strong, even though k_H is known to overpredict k. This finding suggests that previous wind speed/gas exchange parameterizations are unsuitable for the seagrass-dominated area and a specific parameterization for these fetch-limited environments is needed. In the study presented here, a $^3He/SF_6$ tracer release experiment was used to determine k in a shallow seagrass-dominated environment to understand processes that control k and to derive a parameterization for this environment.

2 Methods

2.1 Study site

Florida Bay is located in the southernmost part of Florida, USA. It is situated between the Everglades and the Florida Keys, and covers approximately 2,000 km^2. In this bay, the depth is less than 3.5 m and the canopy length of seagrasses is between 0.08 and 0.2 m (Sogard et al., 1989). *Thalassia testudinum* and *Laurencia* are the dominate seagrass and macroalgae, respectively, in the benthic communities, with an average standing crop of 63.6 and 8.9 g dry weigh m^{-2}, respectively (Zieman et al., 1989). Phytoplankton community is dominated by cyanobacteria, diatom, and dinoflagellates (Philips and Badylak, 1996). Cyanobacteria blooms occur frequently in the central north region of the bay due to nutrient input from the land (Phlips et al., 1999; Lavrentyev et al., 1998). Wind is persistently from southeast to northwest during summer and from north to south during winter (Wang et al., 1994). Current speed is about 0.02−0.14 m s^{-1} (Wang, 1998), and tidal amplitude is affected by the lunar tide which has an amplitude of 0.02−0.04 m (Wang et al., 1994). The $^3He/SF_6$ tracer release experiments were conducted in Florida Bay between 3 and 8 April 2015 near Bob Allen Keys (Fig. 1).

https://doi.org/10.5194/egusphere-2022-525
Preprint. Discussion started: 13 July 2022
© Author(s) 2022. CC BY 4.0 License.

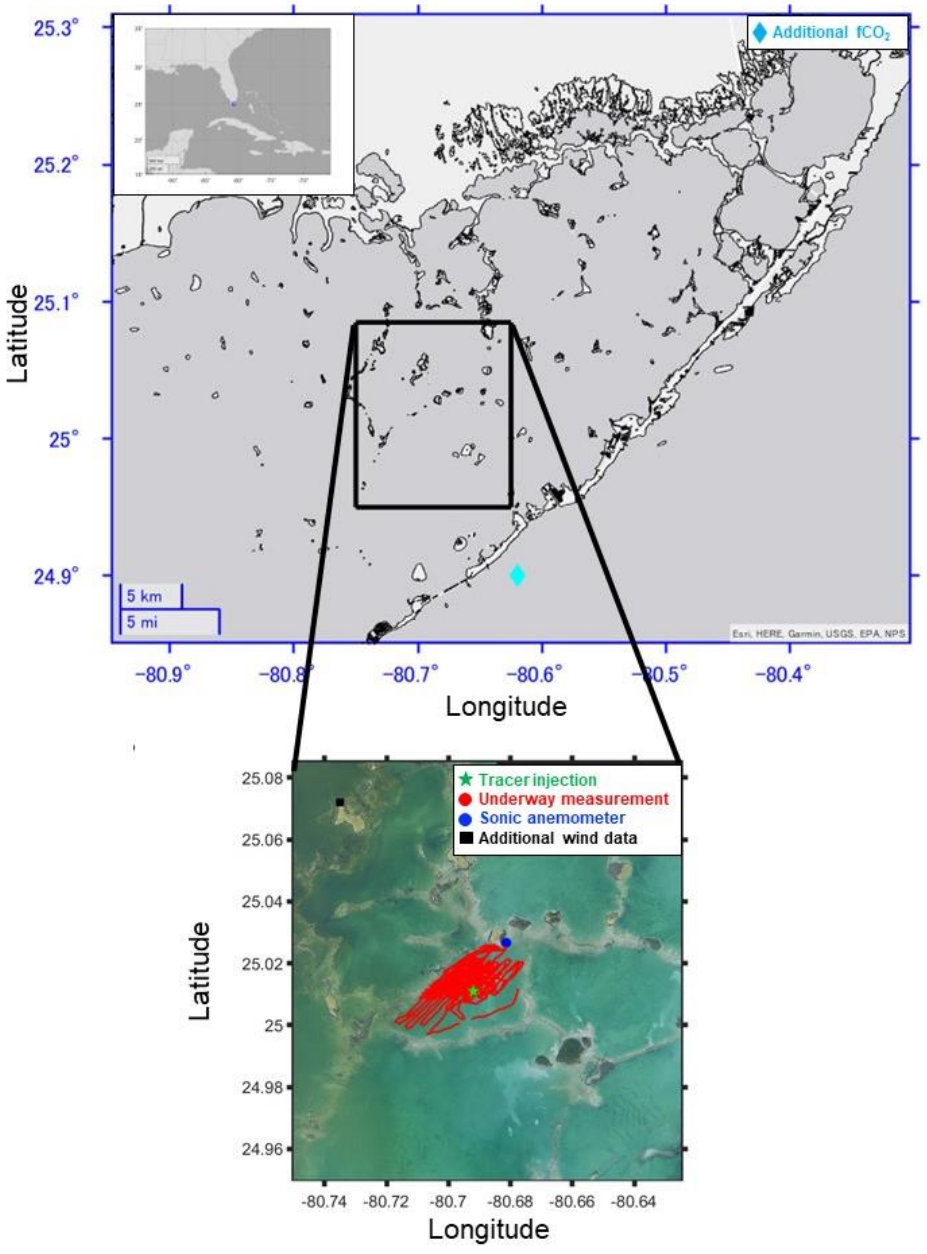

Fig. 1 Map of the study area. Green star, red dots, blue dot, black square, and cyan diamond indicate where ^{3}He and SF_6 were injected, underway measurement was conducted, wind velocity, air temperature, sea temperature, salinity and tidal amplitude were measured, additional wind velocity was measured, and additional fCO_2 were measured. Note that sea temperature, salinity, tidal amplitude and additional wind velocity were taken from Everglades National Park, and additional fCO_2 were taken from NOAA. Map data are generated by MATLAB geobasemap "darkwater" and downloaded from Fish and Wildlife Research Institute (https://myfwc.com/research/) and NOAA (https://www.noaa.gov/)

https://doi.org/10.5194/egusphere-2022-525
Preprint. Discussion started: 13 July 2022
© Author(s) 2022. CC BY 4.0 License.

2.2 Tracer injection and underway SF_6 measurement

We injected ^3He and SF_6 at the study location (25.0107°N, 80.692°W; green star in Fig. 1). The mixture of ^3He and SF_6, at a ratio of 1:340, was injected into the water via a length of diffuser tubing. After the injection, we performed underway SF_6 measurements. An underway SF_6 analysis system (Ho et al., 2002) measured SF_6 concentrations in the surface water every ~45 s. The system is composed of a gas extraction unit and an analytical unit. The gas extraction unit continuously removes SF_6 from the water for measurement using a membrane contactor. The other unit is composed of a gas chromatograph equipped with an electron capture detector (GC/ECD). Based on previous experiments, the system has a detection limit of 1×10^{14} mol L^{-1} and an analytical precision of ±1% (Ho et al., 2018b). A personal computer displayed the SF_6 concentrations in real time. This provided an areal distribution of the SF_6 patch, which guided the boat navigation. Around the center of the patch, we conducted discrete ^3He and SF_6 sampling (see below).

2.3 Discrete ^3He and SF_6 measurements

We collected ^3He samples (ca. 40 mL each) by copper tubes mounted in aluminum channels and sealed at the ends with stainless steel clamps. In the shore-based laboratory at the end of the experiment, ^3He and other gases were extracted from the water in the copper tubes and transferred to flame-sealed glass ampoules. We measured ^3He concentration using a He isotope mass spectrometer (Ludin et al., 1998). Discrete SF_6 samples were taken by 50-mL glass syringes and submerged in water in a cooler until measurement back in the laboratory at the end of each day. SF_6 was extracted by headspace technique and measured on a GC/ECD as described by Wanninkhof et al. (1987).

2.4 measurements of wind, temperature, salinity and tide

We measured wind speed, wind direction, and air temperature at ~5 m above sea level every 10 s using a sonic anemometer near Bob Allen key (25.02663°N, 80.68137°W; blue dot in Fig. 1). The air temperature was averaged every 1 h to calculate the air-sea temperature difference (sea temperature minus air temperature). Hourly tidal amplitude, sea surface temperature, and salinity data from the same site were obtained from Everglades National Park (https://www.ndbc.noaa.gov/). Additional wind speeds measured at ~3 m above the sea level at 25.07209°N, 80.73511°W (black square in Fig. 1) between 2015 and 2019 were obtained from Everglades National Park.

Wind data were extrapolated to 10 m above the sea level using the equation below:

$$u_z = \frac{u_{*a}}{\kappa} \ln\left(\frac{z}{z_0}\right), \quad (1)$$

where u_z is the wind speed at height z, κ is the von Kármán constant (0.4), u_{*a} is the mean frictional wind velocity and z_0 is the roughness length. The roughness length in Florida Bay has been estimated to be in the range of 0.013 and 0.062 m (Cornelisen and Thomas, 2009); we used z_0 of 0.038 m which is an average of those values.

https://doi.org/10.5194/egusphere-2022-525
Preprint. Discussion started: 13 July 2022
© Author(s) 2022. CC BY 4.0 License.

2.5. Underway pCO_2 Measurements

We measured the pCO_2 along the boat truck by an underway system based on the design of Ho et al. (1997) and incorporating the suggestions from Pierrot et al. (2009). Water was pumped through a thermosalinograph (TSG) into a showerhead equilibrator, and a high precision thermistor measured the temperature. The gas was dried by Nafion and $Mg(ClO_4)_2$ dryers, and was continuously circulated through a non-dispersive infrared (NDIR; LI-COR 840A) analyzer. We stopped the flow during measurement and vented the NDIR cell to the atmosphere. Atmospheric air was taken from an inlet at the bow of the boat through a length of aluminum/plastic composite tubing (Dekabon), and was diverted into the NDIR analyzer at specific times. We calibrated the analyzer at regular time intervals with a World Meteorological Organization-traceable CO_2 standard and a CO_2-free reference gas (UHP N_2 passed through soda lime to remove CO_2). With measured xCO_2, barometric pressure (P), and water vapor pressure at water surface temperature (Vp), we calculated the water and atmospheric pCO_2 by applying the following expression (DOE, 1994): $pCO_2 = (P-Vp) \times xCO_2$. pCO_2 values were corrected for temperature shifts in the sample from the intake point (i.e., as measured by the TSG) to the pCO_2 system using an empirical equation proposed by Takahashi et al. (1993). Fugacity of CO_2 (fCO_2) was calculated by $fCO_2=\alpha \times pCO_2$, where α is an activity coefficient calculated from a formula in Wanninkhof and Thoning (1993). Additional fCO_2 data were taken from National Oceanic and Atmospheric Administration (NOAA) (https://www.pmel.noaa.gov/) at 24.90°N, 80.62°W (cyan diamond in Fig. 1). CO_2 flux between air and sea was calculated with solubility (K) and fCO_2 by the equation below:

$$F = k\mathrm{K}(\mathrm{fCO}_{2sea} - \mathrm{fCO}_{2air}), \quad (2)$$

where the K was calculated from the measured temperature and salinity (Weiss, 1974).

2.6. gas transfer velocity measurement

The two tracers, ^3He and SF_6, were injected together into the mixed layer at a constant ratio, and the ratio of $^3He/SF_6$ was measured over time as written above. The technique relies on the well-tested assumption that patch dilution, such as by horizontal mixing, affects the individual tracer concentrations but does not alter the $^3He/SF_6$ ratio; the only process that changes the $^3He/SF_6$ ratio is air-sea gas exchange. The gas transfer velocity for ^3He, $k_{^3He}$, can be determined as follows (Wanninkhof et al., 1993):

$$k_{^3He} = -h\frac{\mathrm{d}}{\mathrm{dt}}\left(\ln\left(\,^3\mathrm{He}_{\mathrm{exc}}/\mathrm{SF}_6\right)/1 - \left(\mathrm{Sc}_{\mathrm{SF}_6}/\mathrm{Sc}_{^3\mathrm{He}}\right)^{-1/2}\right) \quad (3)$$

where h is the measured water depth in Florida Bay, adjusted for tidal variation. $^3He_{exc}$ is the ^3He in excess of solubility equilibrium with the atmosphere (used interchangeably with ^3He here); and Sc_{SF_6} and $Sc_{^3He}$ are the Schmidt numbers (i.e., the kinematic viscosity of water divided by diffusion coefficient of the gas in water) for SF_6 and ^3He, respectively (see section 2.7). The gas transfer velocity measured during this experiment is normalized to $k(600)$, where 600 corresponds to Sc number of CO_2 in freshwater at 20°C:

$$k(600) = k_{^3He}\left(600/\mathrm{Sc}_{^3\mathrm{He}}\right)^{-1/2}. \quad (4)$$

https://doi.org/10.5194/egusphere-2022-525
Preprint. Discussion started: 13 July 2022
© Author(s) 2022. CC BY 4.0 License.

2.7 Calculation of *Sc* number

The *Sc* number is often calculated from a compilation by Wanninkhof (2014). However, since the salinity in Florida Bay is 40, which is higher than the range provided by Wanninkhof (2014), we have re-calculated *Sc* for an extended range here.

In our calculation, the kinematic viscosity for fresh water and seawater are derived from Sharqawy et al. (2010). Molecular diffusion coefficients of various gasses for freshwater were calculated using empirical equations derived from previous studies (Jähne et al., 1987; Wilke and Chang, 1955; Hayduk and Laudie, 1974; King and Saltzman, 1995; Saltzman et al., 1993; Zheng et al., 1998; De Bruyn and Saltzman, 1997). Sulfur hexafluoride (SF_6), methyl bromide (CH_3Br), and trichlorofluoromethane (CFC-11) do not have significant differences in diffusion coefficients between fresh water and a 35 g L^{-1} sodium chloride (NaCl) solution (King and Saltzman, 1995; De Bruyn and Saltzman, 1997; Zheng et al., 1998). However, diffusion coefficients for methane (CH_4), dichlorodifluoromethane (CFC-12), and helium (He) in seawater are 4−7% less than the coefficients for freshwater (Jähne et al., 1987; Saltzman et al., 1993; Zheng et al., 1998). To represent the dependence of molecular diffusion coefficients on salinity for gasses except for SF_6, CH_3Br and CFC-11, we linearly inter/extrapolated the molecular diffusion coefficients for various salinity by assuming that the diffusion coefficients decrease 6 % when salinity is 35 PSU compared with freshwater (Jähne et al., 1987; Wanninkhof, 2014). Molecular diffusion coefficients for a salinity of 40 are about 7% smaller compared with the coefficients for freshwater based on this assumption. Least-squares fourth-order polynomial fit, including the effect of salinity, was produced to predict the *Sc* numbers at various temperatures and salinity (Table 1).

Table 1. Coefficients for a least-squares fourth-order polynomial fit of Schmidt number versus salinity and temperature for various salinity and temperatures from 0 to 40°C.

Gas	**A**	**a**	**B**	**b**	**C**	**c**	**D**	**d**	**E**	**e**	**Sc number (20°C, 0 PSU)**	**Sc number (20°C, 35 PSU)**
^{3}He	334.38	0.90630	-17.566	-0.040902	0.53156	0.0011076	-0.0094081	-1.8342×10^{-5}	7.1715×10^{-5}	1.3483×10^{-7}	132	146
He	377.10	1.1097	-19.810	-0.050665	0.59949	0.0013852	-0.010610	-2.3081×10^{-5}	8.0880×10^{-5}	1.7028×10^{-7}	149	166

https://doi.org/10.5194/egusphere-2022-525
Preprint. Discussion started: 13 July 2022
© Author(s) 2022. CC BY 4.0 License.

Ne	764.44	2.2495	-43.818	-0.11364	1.3943	0.0032933	-0.025331	-5.652×10^{-5}	0.00019561	4.2289×10^{-7}	274	306
Ar	1876	5.5663	-131.69	-0.32458	4.9298	0.010744	-0.099518	-0.00020223	0.00081784	1.5998×10^{-6}	549	619
O_2	1733.6	5.1437	-121.69	-0.29994	4.5556	0.0099283	-0.091963	-0.00018688	0.00075576	1.4784×10^{-6}	507	572
N_2	2080.6	6.1735	-146.06	-0.35999	5.4677	0.011916	-0.11037	-0.00022429	0.00090706	1.7743×10^{-6}	609	687
Kr	2036.2	5.9923	-133.13	-0.35181	4.5886	0.011183	-0.087051	-0.00020169	0.00068746	1.5474×10^{-6}	623	695
Xe	2688.8	7.9128	-181.43	-0.48144	6.3779	0.015655	-0.12233	-0.00028594	0.0009717	2.2082×10^{-6}	788	880
CH_4	1900.3	5.5923	-119.02	-0.31267	3.9947	0.009639	-0.074686	-0.00017095	0.00058531	1.3002×10^{-6}	614	685
CO_2	1914.2	5.6330	-123.18	-0.32481	4.2040	0.010208	-0.079322	-0.00018296	0.00062463	1.3992×10^{-6}	598	667
N_2O	2127	6.3112	-149.31	-0.36802	5.5897	0.012182	-0.11284	-0.00022929	0.0009273	1.8139×10^{-6}	622	702
Rn	3154.1	9.2820	-220.51	-0.58779	7.9274	0.019612	-0.15397	-0.00036344	0.0012313	2.8283×10^{-6}	880	982
SF_6	3024	3.0926	-193.63	-0.14258	6.5878	0.0035655	-0.12409	-5.3058e×10^{-5}	0.00097626	3.5673×10^{-7}	950	996

https://doi.org/10.5194/egusphere-2022-525
Preprint. Discussion started: 13 July 2022
© Author(s) 2022. CC BY 4.0 License.

DMS	258 2.0	7.59 83	- 160.71	- 0.42182	5.373 3	0.0129 46	- 0.10025	- 0.00022905	0.0007 8480	1.7401×10^{-6}	841	938
CFC-12	346 0.3	10.1 83	- 225.72	-0.5963	7.768 8	0.0189 24	- 0.14727	- 0.00034099	0.0011 625	2.6148×10^{-6}	1061	1184
CFC-11	344 6.9	3.52 51	- 214.51	- 0.15589	7.171 7	0.0037 741	- 0.1338	- 5.4896×10^{-5}	0.0010 474	3.6378×10^{-7}	1123	1176
CH_3Br	210 1	2.14 87	- 133.27	- 0.097717	4.508 1	0.0024 177	- 0.084644	- 3.571×10^{-5}	0.0006 6483	2.3896×10^{-7}	668	700
CCl_4	397 3.3	11.7 89	- 278.92	- 0.68747	10.44 2	0.0227 56	- 0.21078	- 0.00042832	0.0017 322	3.3884×10^{-6}	1163	1312

Sc = A+aS + (B+bS)T + (C+cS)T^2 + (D+dS)T^3 + (E+eS)T^4 (T in °C, S in PSU). The last two columns are the calculated Schmidt number for 20°C, 0 PSU and 35 PSU, respectivery. The diffusion coefficients, denominators of *Sc*, are derived from the following: ^{3}He, He, Ne, Kr, Xe, CH_4, CO_2 and Rn measured by Jähne et al. (1987); Ar, O_2, N_2, N_2O, and CCl_4 fit from Wilke and Chang (1955) adapted by Hayduk and Laudie (1974); SF_6 measured by King and Saltzman (1995); DMS measured by Saltzman et al. (1993); CFC-11 and CFC-12 measured by Zheng et al. (1998); CH_3Br measured by De Bruyn and Saltzman (1997). *Sc* numbers for 20°C, 35 PSU become larger than *Sc* numbers for 20°C, 0 PSU by 4.7–4.8% and 10.8–12.8% for SF_6, CFC-11 and CH_3Br and other gasses, respectively. Note that the fits are based on simple assumption (see section 2.7), and the dependence of *Sc* numbers on salinity needs to be investigated more in the future.

2.8 modeling the decrease of ^{3}He/SF_6 ratio

The decrease of the tracer ratio was compared to the decrease predicted by published wind speed/gas exchange parameterizations to assess the validity of these parameterization for the study area. Under the assumption that air-sea gas exchange is the only process that alters the ^{3}He/SF_6 ratio in the water, the change in ^{3}He/SF_6 ratio during this experiment can be modeled by an analytical solution to equation (3):

$$\left({}^3\mathrm{He}/\mathrm{SF_6}\right)_t = \left({}^3\mathrm{He}/\mathrm{SF_6}\right)_{t-1} \exp\left(-\frac{k_{{}^3\mathrm{He}}\Delta t}{h}\left(1-\left(\mathrm{Sc}_{\mathrm{SF_6}}/\mathrm{Sc}_{{}^3\mathrm{He}}\right)^{-1/2}\right)\right) \quad (5)$$

where $(^3\mathrm{He}/\mathrm{SF_6})_t$ is the ^{3}He to SF_6 ratio at time t and $(^3\mathrm{He}/\mathrm{SF_6})_{t-1}$ is the ratio at the previous time step. $k_{{}^3\mathrm{He}}$ is predicted from wind speeds measured during this experiment and existing parameterizations. The skill of the parameterizations to predict

https://doi.org/10.5194/egusphere-2022-525
Preprint. Discussion started: 13 July 2022
© Author(s) 2022. CC BY 4.0 License.

the measured $^3He/SF_6$ during this experiment is evaluated in terms of the coefficient of variation of the root mean square error (cvRMSE):

$$cvRMSE = \frac{\sqrt{\frac{1}{N}\sum_{n=1}^{N}(R_{mod}^{n} - R_{obs}^{n})^2}}{\overline{R_{obs}}}, \quad (6)$$

where R_{obs}^{n} and R_{mod}^{n} are the observed and modeled $^3He/SF_6$ tracer ratios, respectively, and N is the number of stations sampled after the initial sampling (5 in this study). The ability of commonly used parameterizations, including the quadratic relationships of Wanninkhof (1992), Nightingale et al. (2000), and Ho et al. (2006), the exponential relationship of Raymond and Cole (2001), and the hybrid parameterization of Wanninkhof et al. (2009) to predict k in Florida Bay was evaluated by examining the cvRMSE. Equation (6) was also used to evaluate the optimal coefficients (A) for a quadratic ($k = Au_{10m}^2$) parameterization by minimizing the cvRMSE. We regarded A with minimum cvRMSE as the best coefficient for parameterization.

3. Results and discussion

3.1 gas transfer velocity in Florida Bay

The measured $k(600)$ was 4.8 ± 1.8 cm h^{-1} (mean ± s.d.) (Fig. 2), which was lower than previous studies conducted in coastal and open oceans at the same wind speed (Fig. 3 of Ho & Wanninkhof, 2016). A new parameterization was produced based on results from this experiment by minimizing the cvRMSE of $A \cdot u_{10}^2$, where A is a coefficient (Fig. 3):

$$k(600) = 0.125u_{10}^2 \quad (7)$$

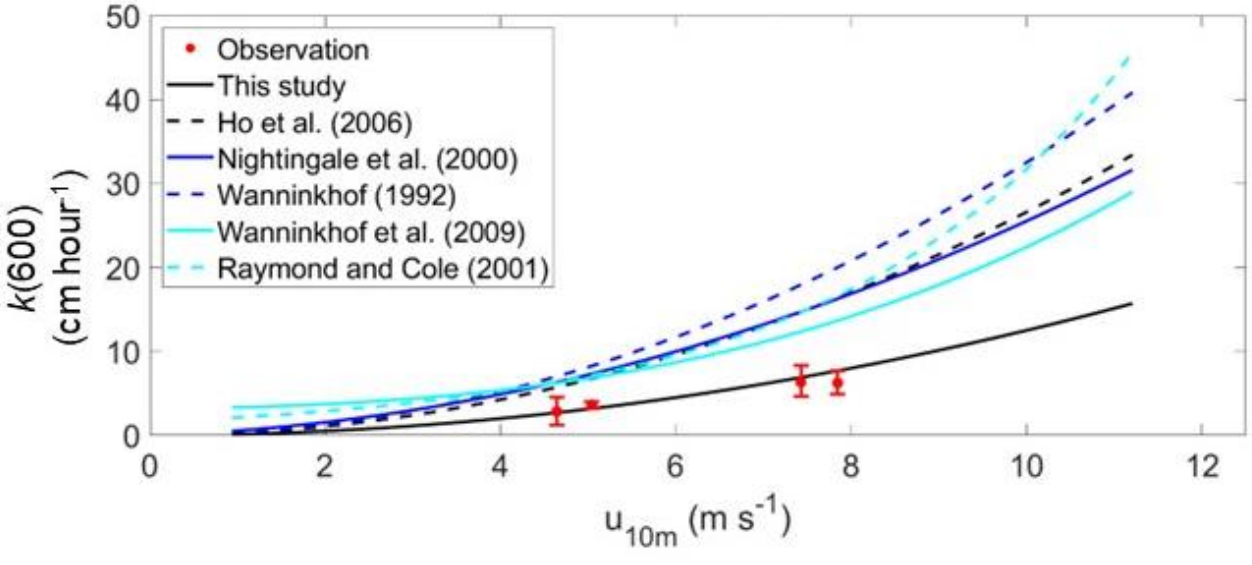

https://doi.org/10.5194/egusphere-2022-525
Preprint. Discussion started: 13 July 2022
© Author(s) 2022. CC BY 4.0 License.

Fig. 2 Measured and modeled *k*(600) (units: cm h^{-1}) with wind speed at 10 m height (units: m s^{-1}).

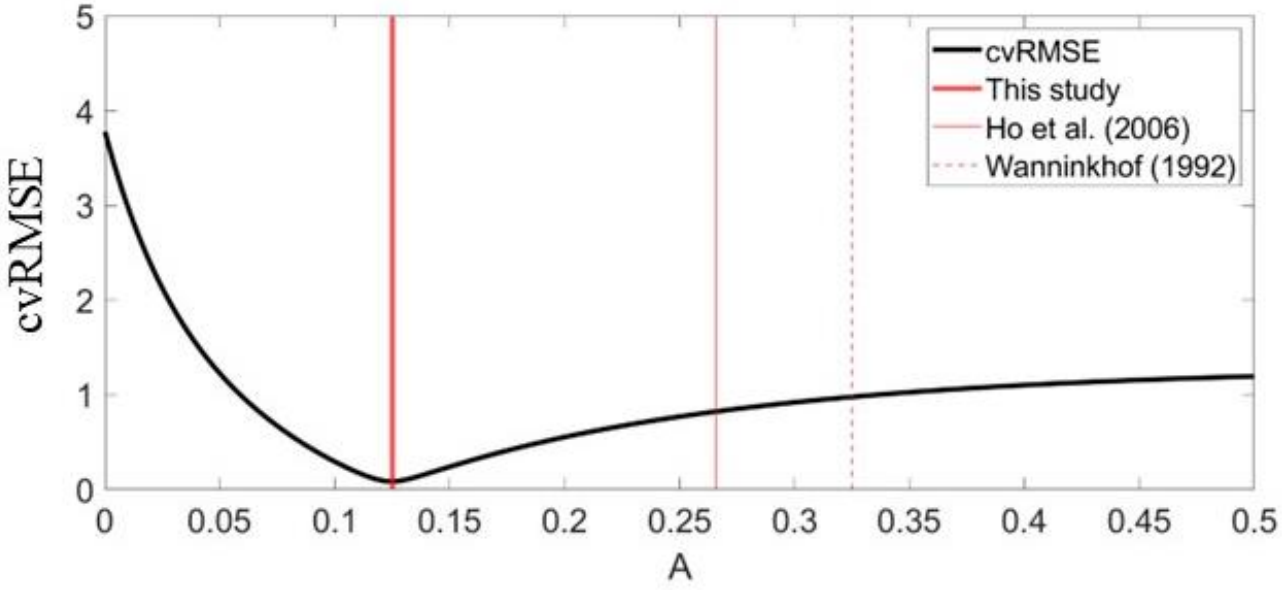

Fig. 3 The relationship between cvRMSE and coefficient, A, in the equation $k(600)=A\ u_{10}^2$. Three vertical lines indicate the coefficients for this study, Ho et al. (2006) and Wanninkhof (1992) from left to right. Note that *k*(660) in Wanninkhof (1992) was converted to *k*(600) by assuming that the ratio of two gas transfer velocities at arbitrary *Sc* number is equal to the ratio of the two *Sc* number to the power of −1/2, like equation (4).

The cvRMSE between the results of this experiment and this new parameterization was 8.6%, while the cvRMSEs calculated from previously published wind speed/gas exchange parameterizations were more than 80% (Table 2). The coefficient of 0.125 was 47% and 38% of the *k*(600) of 0.266 and 0.325 from Ho et al. (2006) and Wanninkhof (1992), respectively (Fig. 3). The result of previous studies which used this parameterization in Florida Bay was modified in section 3.2. *k*(600) between 2015 and 2019 were also calculated using the new parameterization and the previously published parameterizations (Table 3). Using the new parameterization, *k* ranged between 4.2–4.9 cm h^{-1} in this study site between 2015 and 2019.

The deviations of observed $^3He/SF_6$ and modeled $^3He/SF_6$ derived from published parameterizations become larger as time goes, as shown in Figure 4a. This means that the published parameterizations overpredict *k* in Florida Bay, which is consistent with the result of Van Dam et al. (2020). The wind was from the east to west, and wind speed increased towards the latter part of the study period. The mean and the standard deviation of the wind speed during study period was 5.9 ± 2.2 m s^{-1} (range=0.13–13 m s^{-1}). The air-sea temperature difference and tidal amplitude showed diurnal and semidiurnal cycles, respectively.

https://doi.org/10.5194/egusphere-2022-525
Preprint. Discussion started: 13 July 2022
© Author(s) 2022. CC BY 4.0 License.

Table 2. Gas transfer velocities determined from published parameterization.

References	Parameterization	Mean $k(600)$ (cm h^{-1})	cvRMSE
This study	$k(600)= 0.125u_{10}^2$	5.5±3.2	8.6%
Ho et al. (2006)	$k(600)=0.266u_{10}^2$	11.7±6.7	82.5%
Nightingale et al. (2000)	$k(600)=0.333u_{10} + 0.222u_{10}^2$	11.9±6.3	86.6%
Wanninkhof (1992)	$k(660)=0.31u_{10}^2$	14.3±8.2	97.9%
Wanninkhof et al. (2009)	$k(660)=3+0.1u_{10} + 0.064u_{10}^2 + 0.011u_{10}^3$	10.6±4.9	81.2%
Raymond and Cole (2001)	$k(600)=1.58e^{0.3u_{10}}$	12.5±7.2	88.3%

The observed $k(600)$ was 4.8 ± 1.8 cm h^{-1} (average ± standard deviation). Note that $k(660)$ is converted to $k(600)$ by assuming that the ratio of two gas transfer velocities at arbitrary Sc is equal to the ratio of the two Sc to the power of –1/2, like equation (4).

Table 3. Gas transfer velocities of CO_2 in Florida Bay between 2015 and 2019 determined from results presented here and published wind speed/gas exchange parameterization.

References	Mean k (cm h^{-1}) in 2015	Mean k (cm h^{-1}) in 2016	Mean k (cm h^{-1}) in 2017	Mean k (cm h^{-1}) in 2018	Mean k (cm h^{-1}) in 2019	Mean k (cm h^{-1}) between 2015 and 2019
This study	4.2±4.5	4.5±4.7	4.3±6.4	4.5±4.7	4.9±4.9	4.5±5.1
Ho et al. (2006)	8.9±9.7	9.6±10.0	9.2±13.6	9.6±10.0	10.5±10.5	9.6±10.9
Nightingale et al. (2000)	9.2±9.0	9.8±9.3	9.4±12.3	9.9±9.3	10.7±9.7	9.8±10.0
Wanninkhof (1992)	10.9±11.8	11.7±12.2	11.3±16.6	11.8±12.3	12.8±12.9	11.7±13.3
Wanninkhof et al. (2009)	9.4±7.5	9.8±7.8	9.9±14.4	9.8±8.1	10.4±8.4	9.9±9.6
Raymond and Cole (2001)	11.2±14.5	11.8±14.9	19.4±256.1	12.1±17.9	12.9±16.4	13.5±115.6

https://doi.org/10.5194/egusphere-2022-525
Preprint. Discussion started: 13 July 2022
© Author(s) 2022. CC BY 4.0 License.

The mean and standard deviation of wind speed at 10 m height during 2015 and 2019 was 5.0±2.9 m s^{-1}. The standard deviation of Raymond and Cole (2001) became large in 2017 since wind speed was as high as 31.4 m s^{-1}, and k became 2.1×10^4 cm h^{-1}.

Van Dam et al. (2020) estimated the air-sea gas transfer velocity using heat as a proxy (k_H) in Florida Bay. They found that k_H becomes lower than k calculated from published parameterization even though k_H is known to overpredict gas transfer velocity. They suggested that the stratification due to temperature restricts air-sea gas exchange since the deviation between k_H and k from commonly-used parameterization was large when the air-sea temperature difference was large. We examined the relationship between temperature difference and the deviation between observation and the models by calculating cvRMSE in four periods (Figs. 4 and 5). We found no clear relationship between the deviation and air-sea temperature difference. The deviation observed in Van Dam et al. (2020) might be due to the fact that k_H contains the air-sea temperature difference in its equation (equation 7 in Van Dam et al. 2020); k_H becomes smaller when the air-sea temperature difference is large and vice versa. Tidal amplitude was small (~0.1 m) (Fig. 4d), suggesting that tidal velocity was weak and would not have contributed to increasing k.

The new wind speed/gas exchange parameterization predicts the observed change in $^3He/SF_6$ well (Fig. 4a and Table 2), suggesting that wind is the dominant factor controlling gas exchange in this area. In Florida bay, waves are damped by seagrasses (Prager and Halley, 1999), which might be one of the causes of lower k in this study. There is also the possibility that limited wind fetch in this region led to relatively weak waves and turbulence compared to other regions, contributing to lower k. Wind fetch is limited in this region, since the wind mostly blows from east to west, and the Florida Keys restricts the water exchange between the bay and the Atlantic Ocean (Fig. 1 and Fig. 4b).

https://doi.org/10.5194/egusphere-2022-525
Preprint. Discussion started: 13 July 2022
© Author(s) 2022. CC BY 4.0 License.

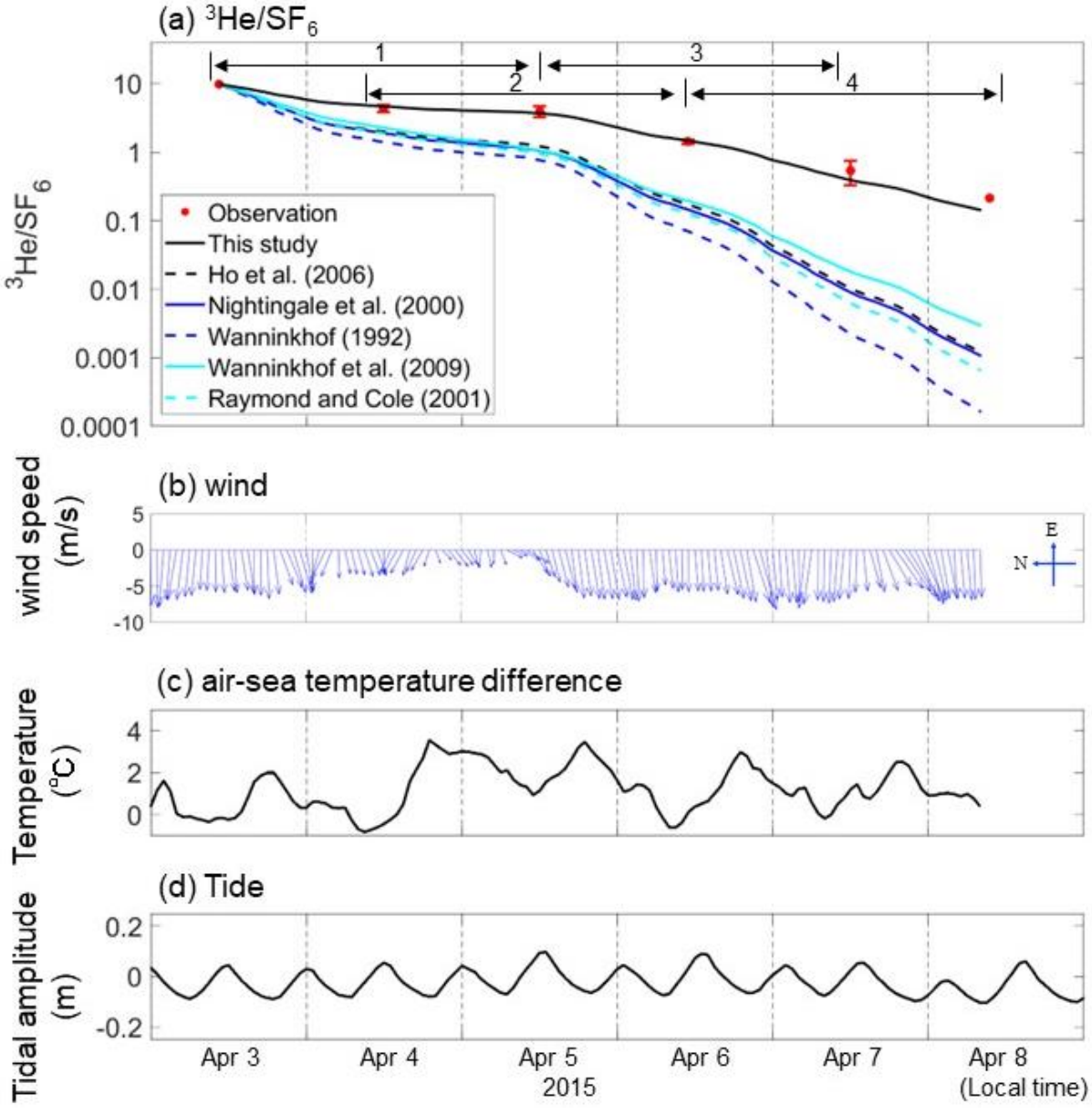

240 **Fig. 4** Time series of (a) measured and modeled change in ^{3}He/SF$_6$, (b) hourly averaged wind vector at 10 m height (units: m s^{-1}), (c) temperature difference (sea temperature minus air temperature; units: °C) and (d) tidal amplitude (units: m). Note that the wind direction is toward north when the vector is toward left. The time zone is local time. The numbers in (a) indicate the periods corresponding to the x-axis in Fig. 5.

https://doi.org/10.5194/egusphere-2022-525
Preprint. Discussion started: 13 July 2022
© Author(s) 2022. CC BY 4.0 License.

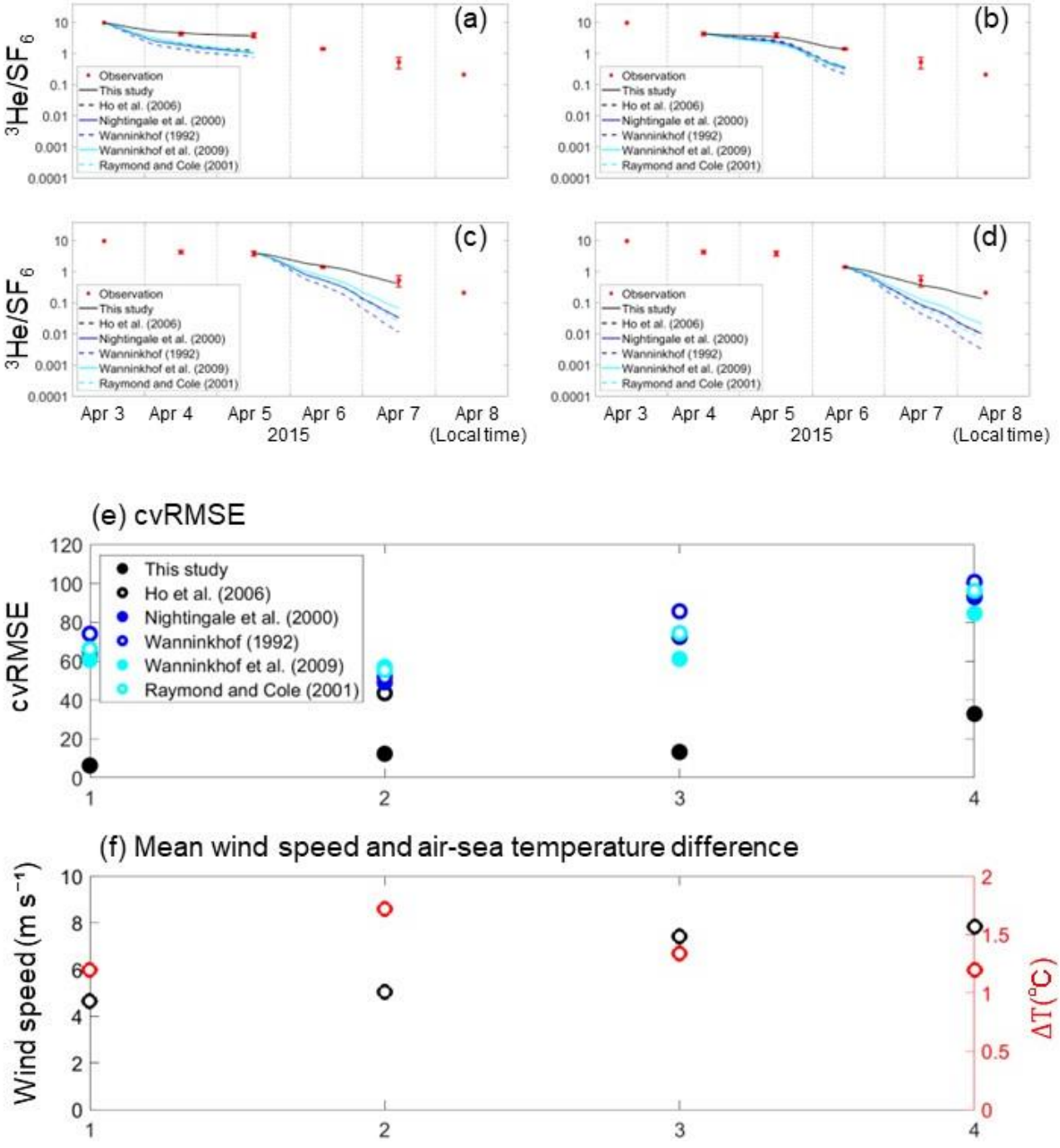

Fig. 5 Time series of measured and modeled change in $^3He/SF_6$ in (a) period 1, (b) period 2, (c) period 3, and (d) period 4 in Fig. 4. $^3He/SF_6$ value is set to the starting point of each period. (e) The cvRMSE, (f) mean wind speed (units: m s^{-1}) and air-sea temperature difference (units: °C) during the period of 1–4. The x-axis represents the periods in Fig. 4a.

https://doi.org/10.5194/egusphere-2022-525
Preprint. Discussion started: 13 July 2022
© Author(s) 2022. CC BY 4.0 License.

3.2 Implications for biogeochemistry

The parameterization determined in this study could be applied to other seagrass ecosystems, since seagrass ecosystems are typically in coastal regions. In these environments, waves are damped by seagrasses and limited fetch. This wind speed/gas exchange parameterization proposed here might be applicable not only in seagrass ecosystems but also in other wind-fetch limited areas. To assess the applicability of this new parameterization in other inland ecosystems, additional $^3He/SF_6$ dual tracer experiments will need to be conducted.

The observed daytime pCO_{2sea} and pCO_{2air} were 228 ± 16 and 393 ± 3 µatm, respectively (Fig. 6a). The pCO_{2sea} of 228 ± 16 µatm was in the range shown by Zhang and Fischer (2014) which examined the pCO_{2sea} in whole basin of the Florida Bay from 2006 to 2012, and showed that pCO_{2sea} minima became ~200 µatm in April (Fig. 3 of Zhang and Fischer 2014). Since the observed pCO_{2sea} was lower than pCO_{2air}, CO_2 goes from air to the sea during the daytime in the observation period (between 3 and 8 April 2015). The calculated CO_2 flux using the measured pCO_2 difference and modeled k in this study was –4.4 ± 2.7 mmol m^{-2} day^{-1} (negative value means CO_2 goes from the air to the sea) (Fig. 6b). Although we did not conduct pCO_2 measurement during the night and so the calculated value is biased toward daytime, the daily averaged pCO_{2sea} and CO_2 flux during the whole observation period would be still lower than pCO_{2air} and negative, respectively, considering that the diurnal amplitude of pCO_{2sea} is 140 µatm in similar season (end of March) in Florida Bay (Yates et al., 2007).

https://doi.org/10.5194/egusphere-2022-525
Preprint. Discussion started: 13 July 2022
© Author(s) 2022. CC BY 4.0 License.

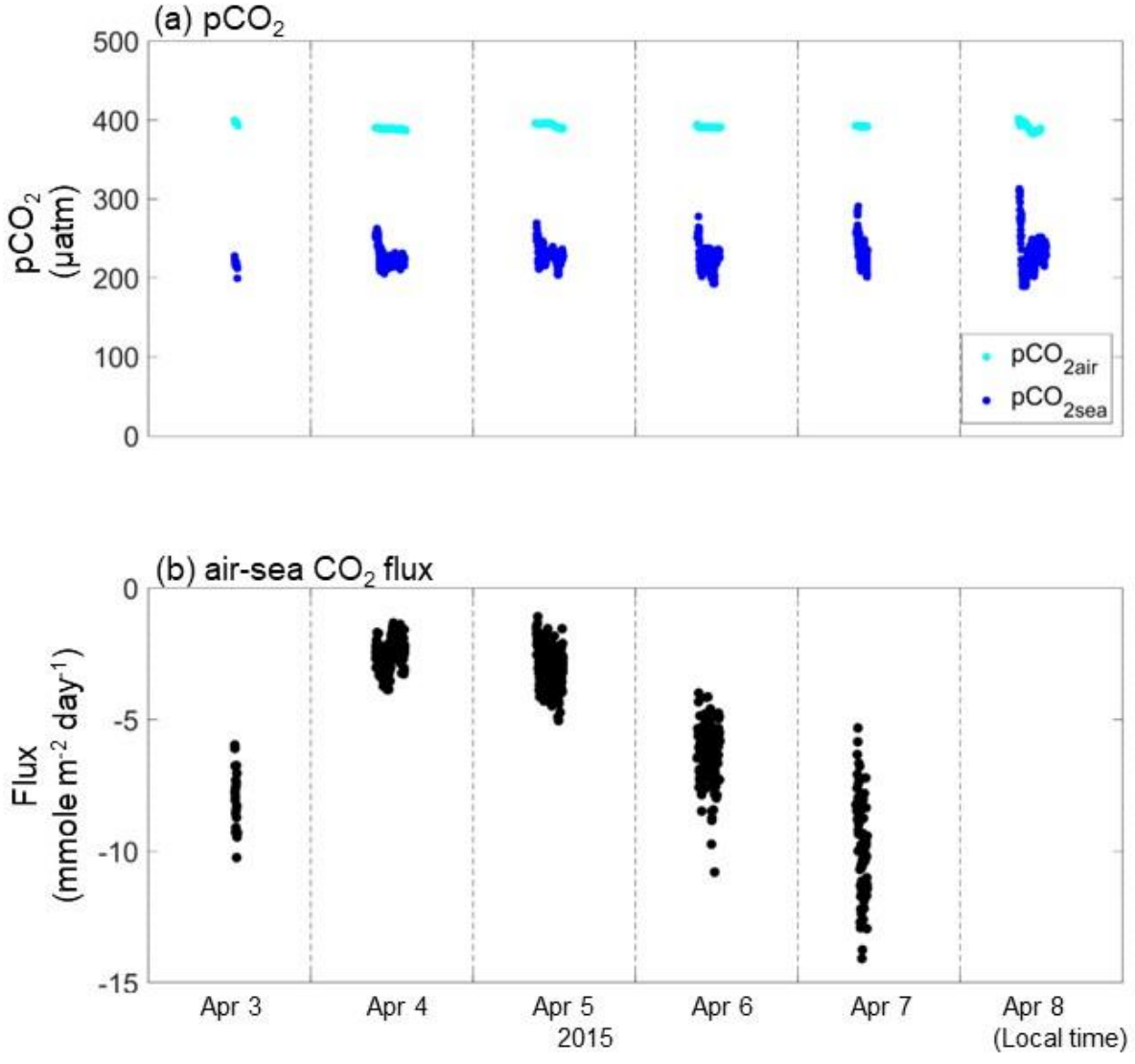

Fig. 6 Time series of (a) measured pCO_{2sea} (blue dots) and pCO_{2air} (cyan dots) (units: µatm), (b) calculated CO_2 flux (units: mmole m^{-2} day^{-1}). The time zone is local time.

Yearly mean CO_2 flux is, however, known to go from the sea to the air in Florida Bay (e.g., Zhang and Fischer, 2014; Van dam et al., 2021). The pCO_2 and CO_2 flux in Florida Bay are suggested to have seasonality due to cyanobacteria blooms (Zhang and Fischer, 2014). CO_2 flux in Florida Bay was estimated to be 3.93 ± 0.91 mol m^{-2} yr^{-1} (Zhang and Fischer, 2014) using the parameterization of Wanninkhof (1992); we recalculated the CO_2 flux to be 1.50 ± 0.35 mol m^{-2} yr^{-1} by multiplying 0.38 (see section 3.1). By conducting atmospheric eddy covariance measurement, Van Dam et al. (2021) showed that the CO_2 flux in Florida Bay is 6.1 mol m^{-2} $year^{-1}$, which is higher than the corrected value of 1.50 ± 0.35 mol m^{-2} yr^{-1} in Zhang

https://doi.org/10.5194/egusphere-2022-525
Preprint. Discussion started: 13 July 2022
© Author(s) 2022. CC BY 4.0 License.

and Fischer (2014). Although the reason is not clear, cyanobacteria bloom might be lower when Van Dam et al. (2021) conducted their observation (2019–2020), resulting in higher CO_2 flux from sea to air, since there is no negative mean CO_2 flux in spring when they conducted measurement (Fig. 1a in Van Dam et al., 2021). Van Dam et al. (2021) also calculated the excess CO_2 in the water in Florida Bay to be between 5.2 and 6.0 μmol kg^{-1}, using a mean k of 11.7 cm h^{-1}, which is the same as k derived from Wanninkhof (1992); they should have used k of 4.5 cm h^{-1} for their calculation (Table 3).

4. Summary

Air-sea gas exchange was investigated in a seagrass ecosystem using the ^3He and SF_6 dual tracer technique. The gas transfer velocity was lower than that in other coastal and open oceans, and commonly-used parameterizations tend to overpredict the gas transfer velocity, especially when wind was relatively strong. New wind speed/gas exchange parameterization was proposed ($k(600) = 0.125u_{10}^2$), which fitted well to the observed gas exchange. This suggests that wind is the dominant factor for the gas transfer velocity in the studied seagrass ecosystem. To assess the applicability of the proposed parameterization, more tracer release experiments are needed at similar inland ecosystems.

Data availability

The data used for this article is found at https://doi.org/10.5281/zenodo.6730934.

Author contributions

DH conceived and designed the experiment. RD performed the analysis.

Competing interests

The authors have declared that they have no competing interests.

Disclaimer

Acknowledgements

The authors thank Nicholas Chow, Nathalie Coffineau, Ben Hickman, Lindsey Visser for assistance in the field, Peter Schlosser for measuring the ^3He samples, Rik Wanninkhof for guidance on the Schmidt number calculations, Damon Rondeau at Everglades National Park for providing data on wind, temperature, salinity, and tide.

https://doi.org/10.5194/egusphere-2022-525
Preprint. Discussion started: 13 July 2022
© Author(s) 2022. CC BY 4.0 License.

Financial support

Funding was provided by the National Aeronautics and Space Administration (NNX14AJ92G).

Review statement

References

Cornelisen, C., and F. Thomas (2009), Prediction and validation of flow-dependent uptake of ammonium over a seagrass-hardbottom community in Florida Bay, Mar. Ecol. Prog. Ser., 386, 71–81.

De Bruyn, W. J., and E. S. Saltzman. (1997). Diffusivity of methyl bromide in water. Mar. Chem. 57:55-59. doi:10.1016/S0304-4203(96)00092-8.

DOE (1994), *Handbook of Methods for the Analysis of the Various Parameters of the Carbon Dioxide System in Sea Water, Version 2*, edited by A. G. Dickson and C. Goyet, ORNL/CDIAC-74.

Duarte, C. M., J. J. Middleburg,and N. Caraco. 2005. Major role of marine vegetation on the oceanic carbon cycle. *Biogeosciences* **2**: 1–8.

Fourqurean, J. W., and others. 2012. Seagrass ecosystems as a globally significant carbon stock. Nat. Geosci. 5: 505–509. doi:10.1038/ngeo1477

Ho, D. T., N. Coffineau, B. Hickman, N. Chow, T. Koffman, and P. Schlosser (2016), Influence of current velocity and wind speed on air-water gas exchange in a mangrove estuary, Geophys. Res. Lett., doi:10.1002/2016GL068727.

Ho, D. T., Engel, V. C., Ferrón, S., Hickman, B., Choi, J., & Harvey, J. W. (2018a). On factors influencing air-water gas exchange in emergent wetlands. Journal of Geophysical Research: Biogeosciences, 123(1), 178–192. https://doi.org/10.1002/2017JG004299

Ho, D. T., Schlosser, P., & Caplow, T. (2002). Determination of longitudinal dispersion coefficient and net advection in the tidal Hudson River with a large-scale, high resolution SF_6 tracer release experiment. *Environmental Science & Technology*, **36**(15), 3234–3241. doi:10.1021/es015814+

Ho, D. T., C. S. Law, M. J. Smith, P. Schlosser, M. Harvey, and P. Hill (2006), Measurements of air-sea gas exchange at high wind speeds in the Southern Ocean: Implications for global parameterizations, Geophys. Res. Lett., 33, L16611, doi:10.1029/2006GL026817.

Ho, D. T., E. H. De Carlo, and P. Schlosser. 2018b. Air-sea gas exchange and CO_2 fluxes in a tropical coral reef lagoon. J. Geophys. Res. Oceans 123: 8701–8713. doi:10.1029/2018JC014423

https://doi.org/10.5194/egusphere-2022-525
Preprint. Discussion started: 13 July 2022
© Author(s) 2022. CC BY 4.0 License.

Ho, D. T. (1997). Measurements of underway fCO2 in the eastern equatorial Pacific on NOAA ships Malcolm Baldridge and Discoverer from February to September, 1994.

Ho, D. T., & Wanninkhof, R. (2016). Air-sea gas exchange in the North Atlantic: 3He/SF6 experiment during GasEx-98. Tellus Series B, 68(1), 30198. https://doi.org/10.3402/tellusb.v68.30198

Howard JL, Creed JC, Aguiar MVP, Fourqurean JW (2017) CO_2 released by carbonate sediment production in some coastal areas may offset the benefits of seagrass "Blue Carbon" storage. Limnol Oceanogr 63: 160–172. doi:https://doi.org/10.1002/lno.10621

Hayduk, & Laudie, H. (1974). Prediction of diffusion coefficients for nonelectrolytes in dilute aqueous solutions. AIChE Journal, 20(3), 611–615. https://doi.org/10.1002/aic.690200329

Jähne, B., Munnich, K. O., Bosinger, R., Dutzi, A., Huber, W., & Libner, P. (1987). On the parameters influencing air-water gas exchange. *Journal of Geophysical Research*, **92**, 1937–1949. https://doi.org/10.1029/JC092iC02p01937

King, D. B., & Saltzman, E. S. (1995). Measurement of the diffusion coefficient of sulfur hexafluoride in water. *Journal of Geophysical Research*, **100**, 7083–7088. https://doi.org/10.1029/94jc03313

Lavrentyev, P. J., H. A. Bootsma, T. H. Johengen, J. F. Cavaletto & W. S. Gardner, 1998. Microbial plankton response to resource limitation: insights from the community structure and seston stoichiometry in Florida Bay, USA. Marine Ecology Progress Series 165: 45–57.

Ledwell, J. R. (1984). The variation of the gas transfer coefficient with molecular diffusivity. In W. Brutsaert, & G. H. Jirka (Eds.), *Gas transfer at water surfaces* (pp. 293–302). Hingham, MA: Reidel. https://doi.org/10.1007/978-94-017-1660-4_27

Ludin, A., Weppernig, R., Bönisch, G., & Schlosser, P. (1998). Mass spectrometric Measurementmeasurement of helium isotopes and tritium in water samples, *Technical Report Rep. 98–6*, 42 pp, Lamont-Doherty Earth Observatory, Palisades, NY.

Nightingale, P. D., G. Malin, C. S. Law, A. J. Watson, P. S. Liss, M. I. Liddicoat, J. Boutin, and R. C. Upstill-Goddard (2000), In situ evaluation of air-sea gas exchange parameterizations using novel conservative and volatile tracers, Global Biogeochem. Cycles, 14, 373–387, doi:10.1029/1999GB900091.

Philips, E. J., and S. Badylak (1996), Spatial variability in phytoplankton standing crop and composition in a shallow inner-shelf lagoon, Florida Bay, Florida, Bull. Mar. Sci., 58, 203–216.

Phlips, E. J., Badylak, S. and Lynch, T. C. (1999) Blooms of picoplanktonic cyanobacterium Synechococcus in Florida Bay, a subtropical inner-shelf lagoon. Limnol. Oceanogr., 44, 1166–1175.

Pierrot, D., Neill, C., Sullivan, K., Castle, R., Wanninkhof, R., Lüger, H., ... & Cosca, C. E. (2009). Recommendations for autonomous underway pCO2 measuring systems and data-reduction routines. *Deep Sea Research Part II: Topical Studies in Oceanography*, *56*(8-10), 512-522.

Prager, E. J.,and R. B. Halley. 1999. The influence of seagrass on shell layers and Florida Bay mudbanks. *Journal of Coastal Research* 15: 1151–1162.

https://doi.org/10.5194/egusphere-2022-525
Preprint. Discussion started: 13 July 2022
© Author(s) 2022. CC BY 4.0 License.

Raymond, P. A., and J. J. Cole (2001), Gas exchange in rivers and estuaries: choosing a gas transfer velocity, Estuaries, 24, 269–274, doi:10.2307/1352954.

Saltzman, E. S., D. B. King, K. Holmen, and C. Leck. (1993). Experimental determination of the diffusion coefficient of dimethylsulfide in water. J. Geophys. Res. 98:16481-16486 doi:10.1029/93JC01858.

Sharqawy, M. H., Lienhard, J. H., & Zubair, S. M. (2010). Thermophysical properties of seawater: a review of existing correlations and data. *Desalination and water treatment*, *16*(1-3), 354-380.

Sogard, Powell, G. V. N., & Holmquist, J. G. (1989). Spatial Distribution and Trends in Abundance Of Fishes Residing in Seagrass Meadows on Florida Bay Mudbanks. Bulletin of Marine Science, 44(1), 179–199.

Takahashi, T., Olafsson, J., Goddard, J. G., Chipman, D. W., & Sutherland, S. C. (1993). Seasonal variation of CO2 and nutrients in the high-latitude surface oceans: A comparative study. *Global Biogeochemical Cycles*, *7*(4), 843-878.

Van Dam, B. R., M.A. Zeller, C. Lopes, A.R. Smyth, M.E. Böttcher, C.L. Osburn, T. Zimmerman, D. Pröfrock, J.w. Fourqurean, H. Thomas Calcification-driven CO_2 emissions exceed "Blue Carbon" sequestration in a carbonate seagrass meadow Res. Square (2021), 10.21203/rs.3.rs-120551/v1

Van Dam, B. R., Lopes, C. C., Polsenaere, P., Price, R. M., Rutgersson, A., & Fourqurean, J. W. (2020). Water temperature control on CO_2 flux and evaporation over a subtropical seagrass meadow revealed by atmospheric eddy covariance. Limnology & Oceanography, 66, 1–18. https://doi.org/10.1002/lno.11620

Wang, J. D., J. van deKreeke, N. Krishnan, D. Smith, Wind and tide response in Florida Bay, *Bull. Mar. Sci.*, **54**, 579–601, 1994.

Wang, J. D., Subtidal flow patterns in western Florida Bay, *Estuarine Coastal Shelf Sci.*, **46**, 901–915, 1998.

Wanninkhof, R., W. E. Asher, D. T. Ho, C. Sweeney, and W. R. McGillis (2009), Advances in quantifying air-sea gas exchange and environmental forcing, Annu. Rev. Mar. Sci., 1, 213–244, doi:10.1146/annurev.marine.010908.163742.

Wanninkhof, R. (1992), Relationship between gas exchange and wind speed over the ocean, J. Geophys. Res., 97, 7373–7381, doi:10.1029/92JC00188.

Wanninkhof, R., Ledwell, J. R., Broecker, W. S., & Hamilton, M. (1987). Gas exchange on Mono Lake and Crowley Lake, California. *Journal of Geophysical Research*, **92**, 14,567–14,580. https://doi.org/10.1029/JC092iC13p14567

Wanninkhof, R., and K. Thoning (1993), Measurement of fugacity of CO2 in surface water using continuous and discrete sampling methods, Mar. Chem., 44, 189–205.

Wanninkhof, R., W. Asher, R. Weppernig, H. Chen, P. Schlosser, C. Langdon, and R. Sambrotto (1993), Gas transfer experiment on Georges Bank using two volatile deliberate tracers, *J. Geophys. Res.*, **98**, 20,237–20,248.

Wanninkhof, R. (2014). Relationship between wind speed and gas exchange over the ocean revisited. *Limnology and Oceanography: Methods*, **12**(6), 351–362. https://doi.org/10.4319/lom.2014.12.351

Weiss, R. F. (1974), Carbon dioxide in water and seawater: The solubility of a nonideal gas, *Mar. Chem.*, **2**, 203–215.

Wilke, & Chang, P. (1955). Correlation of diffusion coefficients in dilute solutions. *AIChE Journal*, *1*(2), 264–270. https://doi.org/10.1002/aic.690010222

https://doi.org/10.5194/egusphere-2022-525
Preprint. Discussion started: 13 July 2022
© Author(s) 2022. CC BY 4.0 License.

Yates, K. K., Dufore, C., Smiley, N., Jackson, C., and Halley, R. B. (2007). Diurnal variation of oxygen and carbonate system parameters in Tampa Bay and Florida Bay. *Mar. Chem.* 104, 110–124. doi: 10.1016/j.marchem.2006.12.008

Zhang, J.-Z., and C. J. Fischer. 2014. Carbon dynamics of Florida Bay: Spatiotemporal patterns and biological control. Environ. Sci. Technol. 48: 9161−9169. doi:10.1021/es500510z

Zheng, M., W. J. De Bruyn, and E. S. Saltzman. (1998). Measurements of the diffusion coefficients of CFC-11 and CFC12 in pure water and seawater. J. Geophys. Res. 103:1375- 1379. doi:10.1029/97JC02761.

Zieman, J. C., J. W. Fourqurean, and R. L. Iverson. 1989. Distribution, abundance and productivity of seagrasses and macroalgae in Florida Bay. Bull. Mar. Sci. 44: 292–311.